

ARMY RESEARCH LABORATORY



A 2-D Axisymmetric Model of a Stretching Jet in ALEGRA

by Müge Fermen-Coker

ARL-TR-3309

September 2004

NOTICES

Disclaimers

The findings in this report are not to be construed as an official Department of the Army position, unless so designated by other authorized documents.

Citation of manufacturers' or trade names does not constitute an official endorsement or approval of the use thereof.

DESTRUCTION NOTICE—When this document is no longer needed, destroy it by any method that will prevent disclosure of its contents or reconstruction of the document.

Army Research Laboratory

Aberdeen Proving Ground, MD 21005-5066

ARL-TR-3309

September 2004

A 2-D Axisymmetric Model of a Stretching Jet in ALEGRA

Müge Fermen-Coker
Weapons and Materials Research Directorate

REPORT DOCUMENTATION PAGE

Form Approved
OMB No. 0704-0188

Public reporting burden for this collection of information is estimated to average 1 hour per response, including the time for reviewing instructions, searching existing data sources, gathering and maintaining the data needed, and completing and reviewing the collection information. Send comments regarding this burden estimate or any other aspect of this collection of information, including suggestions for reducing the burden, to Department of Defense, Washington Headquarters Services, Directorate for Information Operations and Reports (0704-0188), 1215 Jefferson Davis Highway, Suite 1204, Arlington, VA 22202-4302. Respondents should be aware that notwithstanding any other provision of law, no person shall be subject to any penalty for failing to comply with a collection of information if it does not display a currently valid OMB control number.
PLEASE DO NOT RETURN YOUR FORM TO THE ABOVE ADDRESS.

1. REPORT DATE (DD-MM-YYYY) September 2004		2. REPORT TYPE Final		3. DATES COVERED (From - To) 04 - 10, 2004	
4. TITLE AND SUBTITLE A 2-D Axisymmetric Model of a Stretching Jet in ALEGRA				5a. CONTRACT NUMBER	
				5b. GRANT NUMBER	
				5c. PROGRAM ELEMENT NUMBER	
6. AUTHOR(S) Müge Ferme-Coker				5d. PROJECT NUMBER AH80	
				5e. TASK NUMBER	
				5f. WORK UNIT NUMBER	
7. PERFORMING ORGANIZATION NAME(S) AND ADDRESS(ES) U.S. Army Research Laboratory Terminal Effects Division Weapons and Materials Research Directorate ATTN: AMSRD-ARL-WM-TC Aberdeen Proving Ground, MD 21005-5066				8. PERFORMING ORGANIZATION REPORT NUMBER ARL-TR-3309	
9. SPONSORING/MONITORING AGENCY NAME(S) AND ADDRESS(ES) U.S. Army Research Laboratory 2800 Powder Mill Road Adelphi, MD 20783-1145				10. SPONSOR/MONITOR'S ACRONYM(S)	
				11. SPONSOR/MONITOR'S REPORT NUMBER(S) ARL-TR-3309	
12. DISTRIBUTION/AVAILABILITY STATEMENT Approved for public release; distribution is unlimited.					
13. SUPPLEMENTARY NOTES					
14. ABSTRACT This report presents a numerical model of a stretching copper jet, representative of a Viper shaped charge jet at 35 μ s following detonation. A liner collapse and jet formation model is used to extract data for the jet geometry and the axial velocity distribution. Numerical simulations are carried out using ALEGRA (Arbitrary Lagrangian Eulerian General Research Application), and the results are compared to previously published experimental data and numerical results. ALEGRA results at 35 μ s are then corrected to more accurately reflect experimental observations in the new model representing the stretching jet at the point of impact. Sensitivity studies are conducted using the stretching jet model to determine the effects of computational mesh at later times.					
15. SUBJECT TERMS SCJ, shaped charge, ALEGRA, jet formation, particulation					
16. SECURITY CLASSIFICATION OF:			17. LIMITATION OF ABSTRACT SAR	18. NUMBER OF PAGES 58	19a. NAME OF RESPONSIBLE PERSON Müge Ferme-Coker
a. REPORT U	b. ABSTRACT U	c. THIS PAGE U			19b. TELEPHONE NUMBER (Include area code) 410-278-6018

Contents

List of Figures	v
List of Tables	v
Acknowledgments	vii
Summary	1
1. Introduction	3
2. SCJ Formation Model	4
3. Numerical Construction of the Geometry and the Velocity Profile of a Stretching Jet	9
4. Stretching Jet Model Baseline Results and Sensitivity Studies	12
5. Conclusions	19
References	21
Acronyms	23
Appendix A-1. ALEGRA (Version 4.2) Input File Used for Viper SCJ Formation	25
Appendix A-2. Part 1 of Mesh Used to Simulate Shaped Charge Detonation, Liner Collapse, and Jet Formation	29
Appendix A-3. Part 2 of Mesh Used to Simulate Shaped Charge Detonation, Liner Collapse, and Jet Formation	31
Appendix B-1. MATLAB Program to Determine the Jet Shape at 35 μs, Using Extracted Data from ALEGRA Calculations	33
Appendix B-2. The Viper Jet Boundary at 35 μs	35
Appendix C-1. ALEGRA Problem Specification Deck for the Stretching Jet Model	37

Appendix C-2. APREPRO File to Create a Mesh with the FASTQ Tool	41
Appendix C-3. Parameters File Used in Conjunction with the Files Listed in Appendices C-1 and C-2	43
Distribution List	45

List of Figures

Figure 1. Viper shaped charge radiographs at 90 μs , 100 μs , and 110 μs	6
Figure 2. Mesh and initial configuration of Viper shaped charge representation in ALEGRA.	8
Figure 3. Viper jet formation simulation results at 35 μs : (a) radial velocity distribution, (b) axial velocity distribution, (c) void volume fraction, and (d) copper volume fraction.....	8
Figure 4. Use of EnSight line tool to extract data along the length of the jet.....	9
Figure 5. Sample query entity generated using EnSight.....	10
Figure 6. Approximate representation of Viper shaped charge jet at 35 μs following detonation.....	11
Figure 7. Computationally obtained velocity distribution, modified based on experimental results, to represent the axial velocity distribution along the length of the Viper SCJ at 35 μs following detonation.	12
Figure 8. Stretching jet model initial configuration, representing Viper SCJ description at 35 μs	13
Figure 9. Effect of refinement of a square mesh on (a) jet break-up time and (b) number of particles.....	16
Figure 10. Effect of cell aspect ratio ($\Delta y/\Delta x$) on jet break-up time.....	17
Figure 11. Effect of cell aspect ratio ($\Delta y/\Delta x$) on number of particles formed (a) at 85 μs and (b) at 120 μs	17
Figure 12. Effect of cell aspect ratio ($\Delta y/\Delta x$) on preserving the jet tip speed.....	18
Figure 13. Axial velocity distribution for the particulated jet at 120 μs	19

List of Tables

Table 1. Summary of experimental and computational results for Viper SCJ characteristics.	5
Table 2. Summary of mesh sensitivity investigations using the stretching jet model in ALEGRA.	14

INTENTIONALLY LEFT BLANK.

Acknowledgments

The author acknowledges the support of the U.S. Army Research Laboratory, Weapons and Materials Research Directorate, Armor Mechanics Branch for this work; and wishes to thank Mr. Daniel R. Scheffler and Mr. Kent Kimsey for their technical review and valuable suggestions, and Mr. Stephen Schraml and Mr. Richard Summers for engaging in helpful discussions and sharing their relevant experience during the course of this work.

INTENTIONALLY LEFT BLANK.

Summary

In computational studies associated with armor applications, it is desirable to have a numerical representation of a stretching, necking, and particulating shaped charge jet (SCJ) at the time of impact, without having to model the warhead geometry and simulate detonation and jet formation each time a shaped charge jet is fired against armor. The objective of the current study is to address this requirement by developing a numerical representation of a stretching jet that possesses experimentally confirmed jet characteristics at the time of impact, thus allowing its performance against various types of armor to be studied.

In this report, an analytical representation of the geometric shape and axial velocity distribution of a fully formed, stretching Viper SCJ is obtained and studied using ALEGRA (Arbitrary Lagrangian Eulerian General Research Application), a multi-material arbitrary-Lagrangian-Eulerian (MMALE) solid dynamics code being developed by Sandia National Laboratories (SNL), by modeling liner collapse and jet formation to extract the data, and correcting it to reflect the experimental observations more accurately. Sensitivity studies were conducted using this new stretching jet model that represents a Viper SCJ at 35 μs , to determine the effects of computational mesh at later times.

Of the various jet characteristics, the jet tip speed and length were found to be the least mesh dependent, whereas, the breakup time and number of particles were found to be highly mesh sensitive. However, computational jet particulation is largely, if not completely, due to numerical error propagation. Jet breakup may or may not be observed, depending on the mesh selected. The sensitivity study conducted during this research and summarized in this report aimed at developing a better understanding of mesh effects on this numerically observed phenomenon, so that analysts can pick the properties of their mesh based on the desired accuracy of various jet characteristics in the end. In this study, the difference between the experimentally observed and computationally obtained breakup time varied between 6% and 44%, depending on the cell geometry. For cells with an aspect ratio of 5 and higher in the axial direction, jet particulation did not occur.

Using the stretching jet model introduced in this report, the error in ALEGRA jet tip speed prediction (when the jet is fully formed at 35 μs) was reduced from 7% to nearly 0%, as compared to the experimental measurements that included a certain percentage of error itself. Shortly before the jet particulates at 85 μs , the error in tip speed was reduced from 7% to 3-4%, depending on the mesh used. By reducing the jet length predicted by ALEGRA to match the experimentally observed length at 35 μs (thus eliminating the 11% difference between the ALEGRA prediction and the experimental data), the error in jet length at 85 μs was increased from approximately 6% to 11%, with the ALEGRA predictions both being shorter than the length measured at that time.

INTENTIONALLY LEFT BLANK.

1. Introduction

In computational studies associated with armor applications, it is desirable to have a numerical representation of a stretching, necking, and particulating shaped charge jet (SCJ) at the time of impact, without having to model the warhead geometry and simulate detonation and jet formation each time a shaped charge jet is fired against armor. The objective of the current study is to address this requirement by developing a numerical representation of a stretching jet that possesses experimentally confirmed jet characteristics at the time of impact, thus allowing its performance against various types of armor to be studied.

A stretching copper jet model, representative of a Viper SCJ at 35 μ s following detonation, was generated and studied using ALEGRA (Arbitrary Lagrangian Eulerian General Research Application) (Boucheron et. al., 2002). ALEGRA is a multi-material arbitrary-Lagrangian-Eulerian (MMALE) solid dynamics code, featuring strong shock physics and large deformations, being developed by the Sandia National Laboratories (SNL). The ALE (Arbitrary-Lagrangian-Eulerian) algorithm allows the mesh to be Eulerian, Lagrangian, or Arbitrary. Considering the velocities involved, the ALEGRA simulations presented in this report were performed using Eulerian meshes, although this may not be the optimal technique for ALEGRA. ALEGRA supports Eulerian calculations through its rezoning algorithms, while it conducts calculations on a Lagrangian mesh by default. Typically, the computations take several times longer as compared to CTH, an Eulerian code that is widely used for SCJ simulations., and is being developed by SNL (McGlaun et. al., 1990). ALEGRA was the numerical tool of choice for this study, because it allows a velocity gradient along the jet axis, thereby representing a stretching jet. ALEGRA's Magneto-Hydrodynamics (MHD) capability was also a factor in this decision.

A summary of tasks performed to develop and assess the stretching jet model reported herein is as follows:

1. Detonation, liner collapse, and jet formation of a Viper shaped charge were simulated using ALEGRA.
2. The results of the simulation were imported into EnSight⁷¹ (2003), a multi-purpose post-processing tool by Computational Engineering International. Using the EnSight7 line tool feature, output files were obtained by placing the line tool along the length of the jet at each radial location that contained jet material. Data extracted included material volume fraction and velocity along the length of the jet at 35 μ s following detonation, when the jet was fully formed.

¹EnSight is a registered trademark of Computational Engineering International, Inc.

3. Using MATLAB² software (The MathWorks Inc., 1997), the extracted data was processed to obtain a geometric description of the jet. The resulting processed data was further manipulated using Microsoft Excel³.
4. The tip velocity obtained numerically was adjusted using experimental results; and an analytical formula for the jet shape, as well as the axial velocity gradient, were obtained.
5. A new model was created using formulas developed for the geometry and the adjusted velocity, representing the stretching viper jet when it was fully formed at 35 μ s.
6. The baseline results are compared to experimental results.
7. Mesh dependency of jet tip speed, breakup time, and the number of particles were investigated.

The procedure and results are detailed in the following sections.

2. SCJ Formation Model

As a first step in developing a stretching jet model, a Viper liner collapse and jet formation model was studied using ALEGRA by comparing the results to previously published experimental and numerical data. The Los Alamos National Laboratory (LANL) and SNL experimental data, and SNL computational results obtained using CTH, are reported in Kmetyk et. al., 1991. Their results are summarized in table 1, along with the results obtained during the course of this study, using an identical mesh for ALEGRA. The characteristics of the mesh used are detailed in Kmetyk et. al. (1991) and summarized below for readers' convenience:

- A total of 82 cells in radial direction and 512 cells in axial direction.
- In the radial direction, from the axis of symmetry to 3.5 cm, 70 cells of 0.05 cm width, followed by 12 cells uniformly increasing in width at a 16% rate, up to 5cm.
- In the axial direction, starting from the lower end, 32 cells decreasing in height at 5% rate from 0.25 cm to 0.05 cm up to 4 cm; 70 by 200 square cells of 0.05 by 0.05 cm in size, used in the jet formation region between 4 cm and 14 cm; 80 cells increasing in height at a 2% rate from 0.05 to 0.25 cm up to 24 cm; and 70 by 200 cells with an aspect ratio of 5 (0.05 cm radially, 0.25 cm axially) in the jet elongation region between 24 and 74 cm.

²MATLAB is a trademark of The MathWorks, Inc.

³Microsoft is a registered trademark of Microsoft Corp. in the U.S. and other countries. Microsoft Excel is a product name of Microsoft Corp.

The user-specified options for CTH and ALEGRA runs were almost identical, with the exception that the High-Resolution Interface Tracker (HRIT) was used in the CTH run, as opposed to the Sandia Modified Youngs' Reconstruction Algorithm interface tracker that was used in ALEGRA. The ALEGRA input file used for Viper SCJ formation simulation was based on an SNL-developed model and is listed in appendix A-1. The input file specifies physics, geometry, material insertion, boundary re-mesh control, boundary conditions, as well as the material models. A two-dimensional (2-D) axisymmetric cylindrical geometry was used. The equation of state (EOS) for the copper liner, was defined by table number 3331 in the ANEOS (Analytic EOS) file (Boucheron et. al., 2002; Thompson, 1972, 1973). An elastic plastic constitutive model that uses a generalized Hooke's Law for elastic stress-strain response, von Mises yield criteria, fully isotropic hardening, and simple radial return was used for copper, with the following material properties: Young's modulus = 1.2×10^{12} dynes/cm², Poisson's ratio = 0.33, Yield stress = 3.5×10^9 dynes/cm², and Density = 8.94 g/cm³. The Jones-Wilkins-Lee (JWL) (Lee et. al., 1968) EOS for high explosives was used for LX-14. The density for LX-14 was set to 1.835 g/cm³. The Poisson's ratio for copper was set to 0.33 for ALEGRA, which is different from the 0.345 ratio for CTH as reported by Kmetyk et. al. (1991). This is due to element inversion errors observed in ALEGRA when Poisson's ratio was set to a value higher than 0.33.

Table 1. Summary of experimental and computational results for Viper SCJ characteristics.

Time (μs)	Experimental Data								Computational Results					
	LANL *				SNL *				CTH (SNL computed) *			ALEGRA		
	Length (cm)	Min. Jet Dia. (cm)	Max. Tip Dia. (cm)	Tip Vel. (km/s)	Length (cm)	Min. Jet Dia. (cm)	Max. Tip Dia. (cm)	Tip Vel. (km/s)	Length (cm)	Jet Dia. (cm)	Tip Vel. (km/s)	Length (cm)	Jet Dia. (cm)	Tip Vel. (km/s)
35	20.3 total 13.2 jet	0.3	0.65	9.17	n/a	n/a	n/a	n/a	20.7 total 13.7 jet	0.3 min (0.55 tip)	9.0	21 total 14.6 jet	0.2 min (0.5 tip)	8.6
65	38.1 jet	0.25	0.7	9.18	n/a	n/a	n/a	n/a	38.75	0.25 min 0.51 tip	9.0	37 jet	0.2 (min cell size) min (0.5 tip)	8.6
67.5	n/a	n/a	n/a	n/a	41.6	0.25	0.64	9.26						
75	49.6	0.2	0.55	9.19	n/a	n/a	n/a	n/a	46.5	0.2 min 0.48 tip	9.0	44	0.2 (0.5 tip)	8.6
77.5	n/a	n/a	n/a	n/a	49.4	0.23	0.56	9.2						
85	54.1	0.15	0.5	9.19	n/a	n/a	n/a	n/a	54.5	0.2 0.45 tip	9.0	51.2	0.2 (0.5 tip)	8.6
87.5	n/a	n/a	n/a	n/a	58.1	0.25	0.53	9.16	58.0	0.2min 0.45tip	9.0	52.7	0.2 (0.5 tip)	8.6

NOTE: Dia = diameter; Vel = velocity; and min = minimum.

* From (Kmetyk et. al., 1991)

Note that the LANL and SNL experimental results (Kmetyk et. al., 1991) summarized in table 1 correspond to times prior to jet particulation. Results of several tests conducted by the U.S. Army Research Laboratory (ARL) that correspond to times immediately prior to jet particulation and afterwards are available. A sample set of Viper SCJ radiographs obtained at ARL is shown

in figure 1. At 90 μ s, severe necking was observed for the two-thirds of the length of the jet towards the tip, and particulation was imminent. At 100 μ s and 110 μ s, particulation was progressively more visible, especially towards the tip. At 110 μ s, the jet length was 60.8 cm and the tip speed was 9.3 km/s. The average diameter of the jet was 0.18 cm, and 0.6 cm was the largest diameter at the tip. The errors in tip speed and jet length measurements were estimated to be less than 2%, whereas errors in diameter measurements were typically higher—5% to 40%. Kmetyk et. al. (1991) provides the description and depiction of jet length measurements listed in table 1.

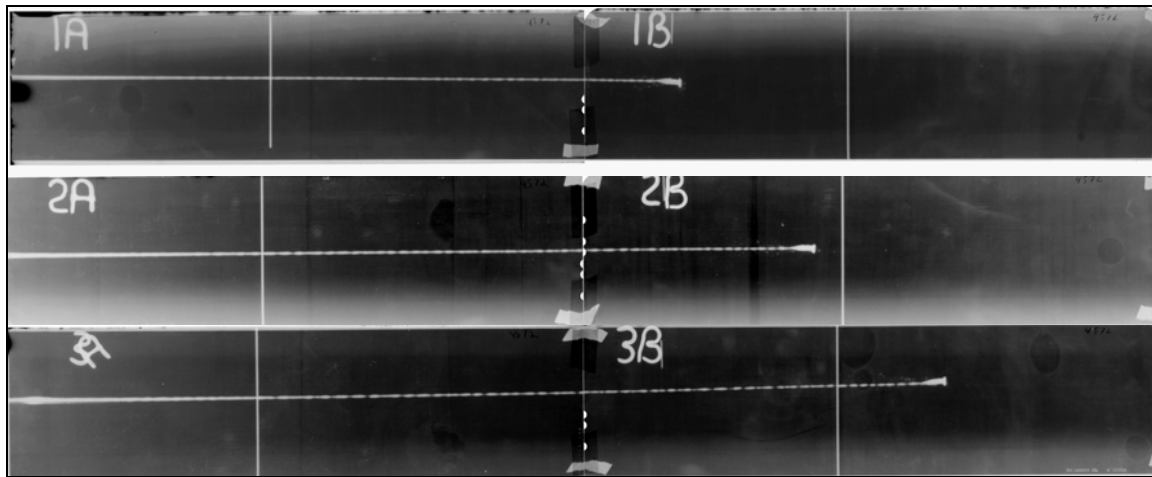


Figure 1. Viper shaped charge radiographs at 90 μ s, 100 μ s, and 110 μ s.

Examining the data presented in table 1, it is observed that both CTH and ALEGRA under-predict the jet tip speed and over-predict the jet length at 35 μ s, as compared to experimental results. The error in jet tip speed for ALEGRA was approximately 6% and was larger than the 2% error for CTH. Since the jet tip had reached its asymptotic velocity at 30 μ s, this error remained relatively constant at later times. At 35 μ s, the error in jet length for ALEGRA was 10.6%, which once again was larger than the error for CTH (3.8%), as compared to the LANL experimental observations. At later times, the over-prediction in jet length gradually dissolved. Note that the CTH results consistently matched the experimental results more closely, compared to the ALEGRA results. The model developed in this report attempts to correct the jet description in terms of geometry and velocity, especially for ALEGRA, based on experimental observations.

Several numerical tests were performed using the computational grid described above in ALEGRA to assess the effect of user-specified options on jet characteristics, although this was not one of the prime objectives of this study. When the detonation point was changed to detonation line, the tip speed dropped to 8.4 km/s, resulting in a shorter jet. At outer radius of the jet however, the velocities were higher. Perhaps consequently, necking was observed to be reduced towards the tip. The tail radius was slightly wider with lower material fraction regions

toward the centerline of the jet. When the constitutive model for copper was changed from elastic plastic to Johnson-Cook (Johnson and Cook, 1983), warnings for negative temperatures and zero or negative energies were significantly increased. Necking was significantly reduced along the length of the jet, and velocities were lower at the jet tail and around the outer diameter of the jet. In addition to changing the constitutive model, when Poisson's ratio was increased from 0.33 to 0.34, element inversion errors were received. Changing the EOS from programmed burn JWL (Lee et. al., 1968) to KEOS JWL (Kerley, 1998) did not cause any significant changes in the results. The tip speed obtained was approximately 8.6 km/s for all the simulations described above. Tail velocities measured by LANL and SNL were approximately 1.81 km/s and 2.2 km/s, respectively (Kmetyk et. al., 1991), whereas the tail velocity obtained using ALEGRA was approximately 1.5 km/s

Using the computational grid described above, the number of cells across the radius dropped to a single cell at times, as the jet stretched. In order to get a better description of the shape of the jet, a more refined mesh was used. To reduce computational time, a thin, long mesh placed on top of a wider block was used so that the detonation could occur in the lower, wider portion of the mesh, allowing the stretching jet to be captured in the long, thin portion. For preprocessing, FASTQ, a 2-D meshing tool, was used (Blacker, 1988). Two FASTQ files were used for these two blocks of mesh, that were then stitched using GJOIN, a program in the Sandia National Laboratories Engineering Analysis Code Access System that combines two or more meshes written in the GENESIS mesh database format into a single mesh (Sjaardema, 1992a).

Appendix A.2 lists the FASTQ input file for the lower part of the mesh that contained the warhead. The mesh extended 10 cm horizontally in x -direction and 30 cm vertically in y -direction. The corners of the rectangular mesh were located at (0,-10), (10,-10), (10,20), and (0,20). The mesh was square between the axis of symmetry ($x = 0$) and 1 cm outward radially ($x = 1$), with a cell size of 0.4 mm in each direction. While the cell size was kept constant along the length of the jet at 0.4 mm, it was expanded radially between $x = 1$ and $x = 10$, from approximately 0.4 mm to 0.6 mm. The FASTQ input file for the thinner part of the mesh is listed in appendix A-3. It extended radially from $x = 0$ to $x = 1$ and axially from $y = 20$ to $y = 120$ to capture the stretching and particulating jet at later times. The cells were uniform: 0.04 by 0.033 cm.

After converting the two FASTQ files listed in appendices A-2 and A-3 into the GENESIS file format, they were combined using GJOIN to create the aggregate mesh (shown in fig. 2) that contains a total of 108,750 cells. Note that, displacement in x -direction is not allowed along the axis of symmetry ($x = 0$), and void is assumed to exist outside all other mesh boundaries.

Figure 3 depicts the ALEGRA predictions of radial and longitudinal velocities, as well as the void and copper volume fractions at 35 μ s. At 90 μ s, the jet tip velocity was 8.7 km/s, approximately the same as the velocity obtained using the coarser mesh discussed above. The jet length was approximately 54 cm at 87.5 μ s, similar to the previously obtained value using ALEGRA, but shorter than the reported CTH and experimental results, i.e. 58 cm (Kmetyk et. al., 1991).

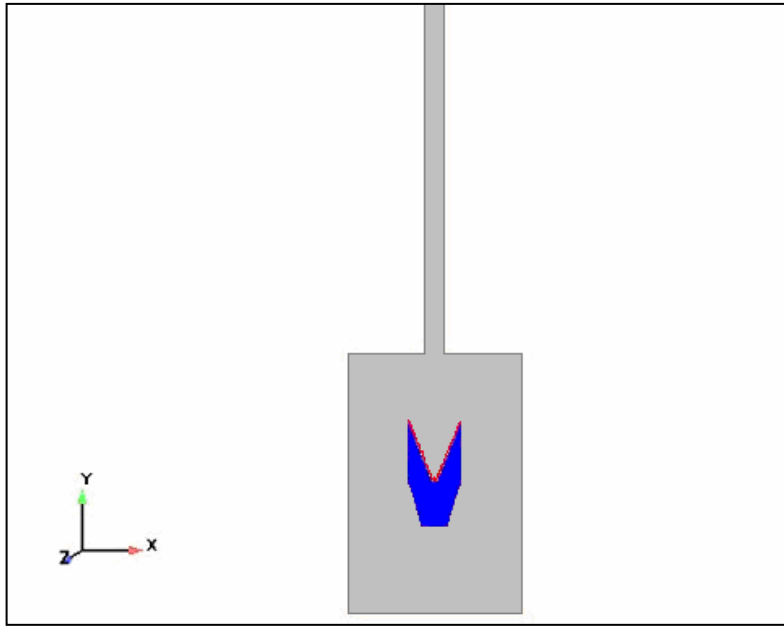


Figure 2. Mesh and initial configuration of Viper shaped charge representation in ALEGRA.

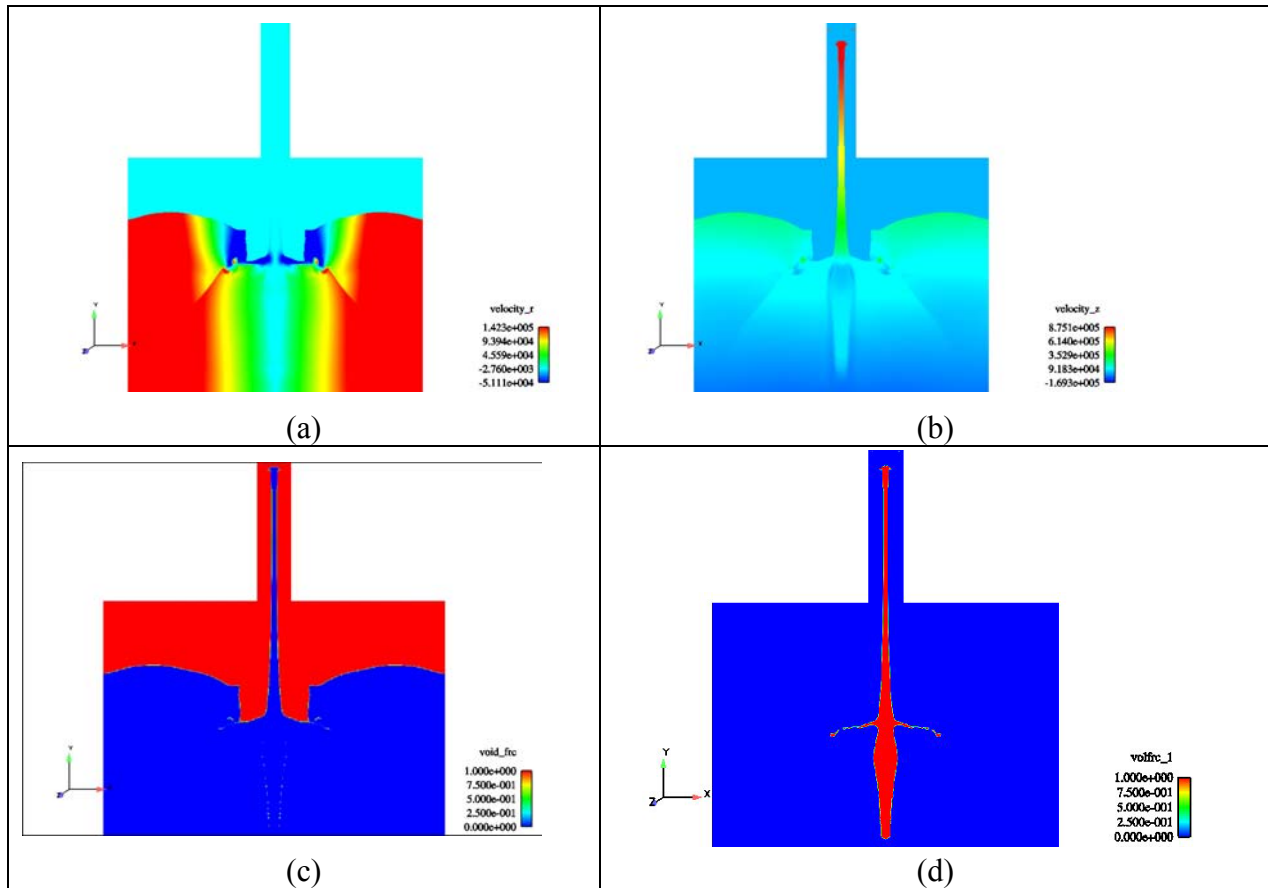


Figure 3. Viper jet formation simulation results at 35 μ s: (a) radial velocity distribution, (b) axial velocity distribution, (c) void volume fraction, and (d) copper volume fraction.

3. Numerical Construction of the Geometry and the Velocity Profile of a Stretching Jet

Once the simulation results depicting liner collapse and jet formation were obtained, as described in section 2, the output file was imported into EnSight (EnSight User Manual, 2003). Then, a data query was performed over distance using the line tool. The line tool was first placed along the axis of symmetry, with its origin located at mesh point labeled “1” in figure 4 and its tip was located at the tip of the jet (not shown in fig. 4). The component of velocity in vertical direction along the jet length and the copper volume fraction were extracted and saved into a text file. The line tool was then moved to each successively labeled mesh point (see fig. 4) parallel to the jet axis, and the data query procedure was repeated. Hence, in this particular example, 18 text files were created. A portion of a sample file that contains the extracted data is shown in figure 5.

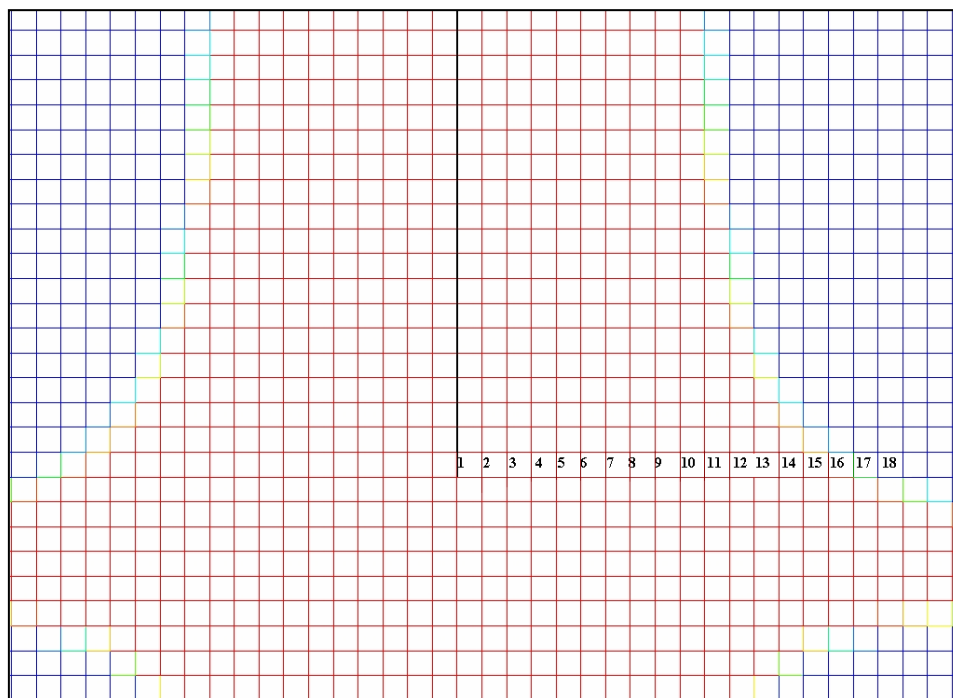


Figure 4. Use of EnSight line tool to extract data along the length of the jet.

VELOCITY_Z vs. VOLFR1 for line tool				
VELOCITY_Z	VOLFR1	X	Y	Z
1.55482e+05	1.00000e+00	0.00000e+00	1.32800e+01	0.00000e+00
1.58690e+05	1.00000e+00	0.00000e+00	1.32947e+01	0.00000e+00
1.61898e+05	1.00000e+00	0.00000e+00	1.33094e+01	0.00000e+00
1.65069e+05	1.00000e+00	0.00000e+00	1.33241e+01	0.00000e+00
1.68145e+05	1.00000e+00	0.00000e+00	1.33388e+01	0.00000e+00
1.71221e+05	1.00000e+00	0.00000e+00	1.33535e+01	0.00000e+00
1.74212e+05	1.00000e+00	0.00000e+00	1.33682e+01	0.00000e+00
1.77136e+05	1.00000e+00	0.00000e+00	1.33829e+01	0.00000e+00
1.80060e+05	1.00000e+00	0.00000e+00	1.33976e+01	0.00000e+00
1.82845e+05	1.00000e+00	0.00000e+00	1.34123e+01	0.00000e+00
1.85603e+05	1.00000e+00	0.00000e+00	1.34270e+01	0.00000e+00
1.88341e+05	1.00000e+00	0.00000e+00	1.34417e+01	0.00000e+00
1.90924e+05	1.00000e+00	0.00000e+00	1.34564e+01	0.00000e+00
1.93507e+05	1.00000e+00	0.00000e+00	1.34711e+01	0.00000e+00
1.96020e+05	1.00000e+00	0.00000e+00	1.34858e+01	0.00000e+00
1.98425e+05	1.00000e+00	0.00000e+00	1.35005e+01	0.00000e+00
2.00830e+05	1.00000e+00	0.00000e+00	1.35152e+01	0.00000e+00
2.03116e+05	1.00000e+00	0.00000e+00	1.35299e+01	0.00000e+00
2.05344e+05	1.00000e+00	0.00000e+00	1.35446e+01	0.00000e+00
2.07573e+05	1.00000e+00	0.00000e+00	1.35593e+01	0.00000e+00
2.09640e+05	1.00000e+00	0.00000e+00	1.35740e+01	0.00000e+00
2.11600e+05	1.00000e+00	0.00000e+00	1.35887e+01	0.00000e+00

Figure 5. Sample query entity generated using EnSight.

A MATLAB program was written to extract the jet shape from the series of text files generated using EnSight. The program, listed in appendix B-1, assumes that the text files are named in a certain format (see the comments in app. B-1 for details). Upon execution of the program, the user is asked to enter the filename and the total number of files to be read. The output is an array “B” that contains the coordinates of the mesh points around the boundary of the jet, defining the jet shape. The shape extracted for the Viper SCJ is listed in appendix B-2. The curvature of the jet boundary may be approximated, as shown in figure 6. A fitted polynomial representation of the jet shape at 35 μs after detonation, when it is fully formed, is

$$z = -4644.2 * r^5 + 10582.0 * r^4 - 9473.5 * r^3 + 4176.8 * r^2 - 915.87 * r + 81.852 \quad (1)$$

where, z is the distance from the tail in centimeters and r is the radial distance from the axis of symmetry. The tail and the tip of the jet correspond to z = 0 and z = 13.2 cm, respectively.

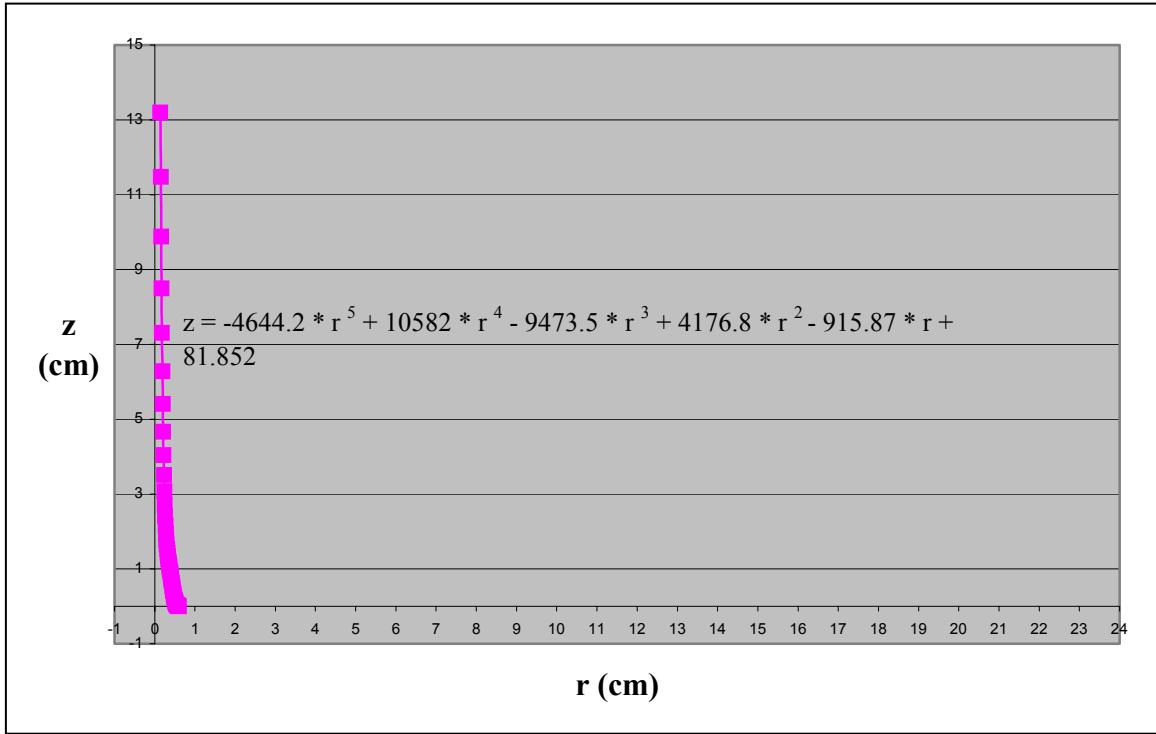


Figure 6. Approximate representation of Viper shaped charge jet at 35 μ s following detonation.

As shown in figure 5, the extracted computational data also includes the velocities computed along the jet length. As previously discussed in section 2, the axial velocities ALEGRA predicted were lower than the observed experimental values and the CTH predictions. To minimize the error in initial conditions for the stretching jet model, the computed velocities were adjusted based on experimental results to provide a better representation of the jet at 35 μ s. The polynomial representation of the modified velocity distribution is

$$V_z = 0.6261 * z^5 - 42.871 * z^4 + 838.0 * z^3 - 7904.5 * z^2 + 93790.0 * z + 182688 \quad (2)$$

where, z represents the distance from the tail as defined in eq 1 and V_z is the corresponding velocity in the positive z direction, along the axis of symmetry. Note that, variation in velocities in the radial direction is ignored. Besides being negligible as compared to the velocities in the z -direction, the radial variation presently cannot be modeled in ALEGRA. The modified velocity distribution at 35 μ s, as compared to the original output from ALEGRA, is shown in figure 7.

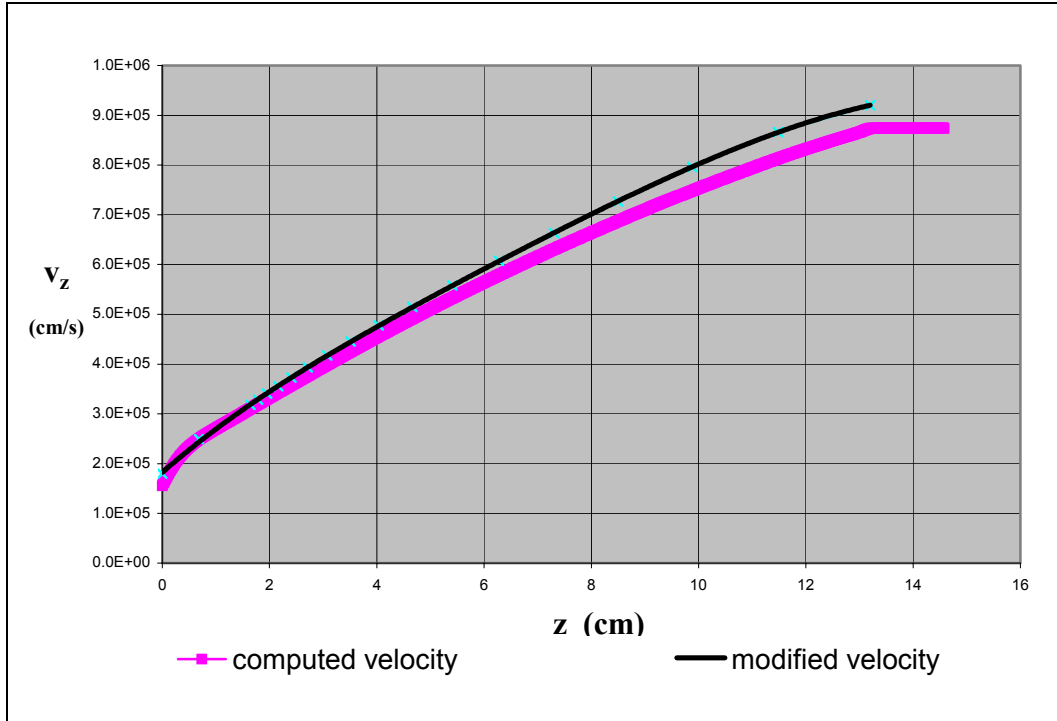


Figure 7. Computationally obtained velocity distribution, modified based on experimental results, to represent the axial velocity distribution along the length of the Viper SCJ at 35 μ s following detonation.

4. Stretching Jet Model Baseline Results and Sensitivity Studies

The jet shape and the modified velocity distribution obtained (as described in sec. 3) represent a stretching Viper SCJ at 35 μ s after detonation. The input file that contains the stretching jet baseline model and uses the APREPRO preprocessing utility (Sjaardema, 1992b) is listed in appendix C-1. APREPRO is an algebraic preprocessor that reads a file that contains general text, as well as algebraic, string, or conditional expressions. It interprets the expressions and outputs them to a file, along with the general text. A mesh input that also uses the APREPRO utility is provided in appendix C-2. A sample of parameters used in both files listed in appendices C-1 and C-2 are listed in appendix C-3. The initial configuration of the new computational model is shown in figure 8. The jet length was 13.2 cm with a minimum tip diameter of 0.14 cm. This configuration ignores the enlarged diameter of the tip of the actual jet. Consequently, if penetration of this jet against a target is considered, the diameter of the crater due to the impact of the tip of the jet would be less than the diameter observed experimentally. The tip velocity was 9.2 km/s and the tail velocity was 1.95 km/s, i.e. the same as observed experimentally.

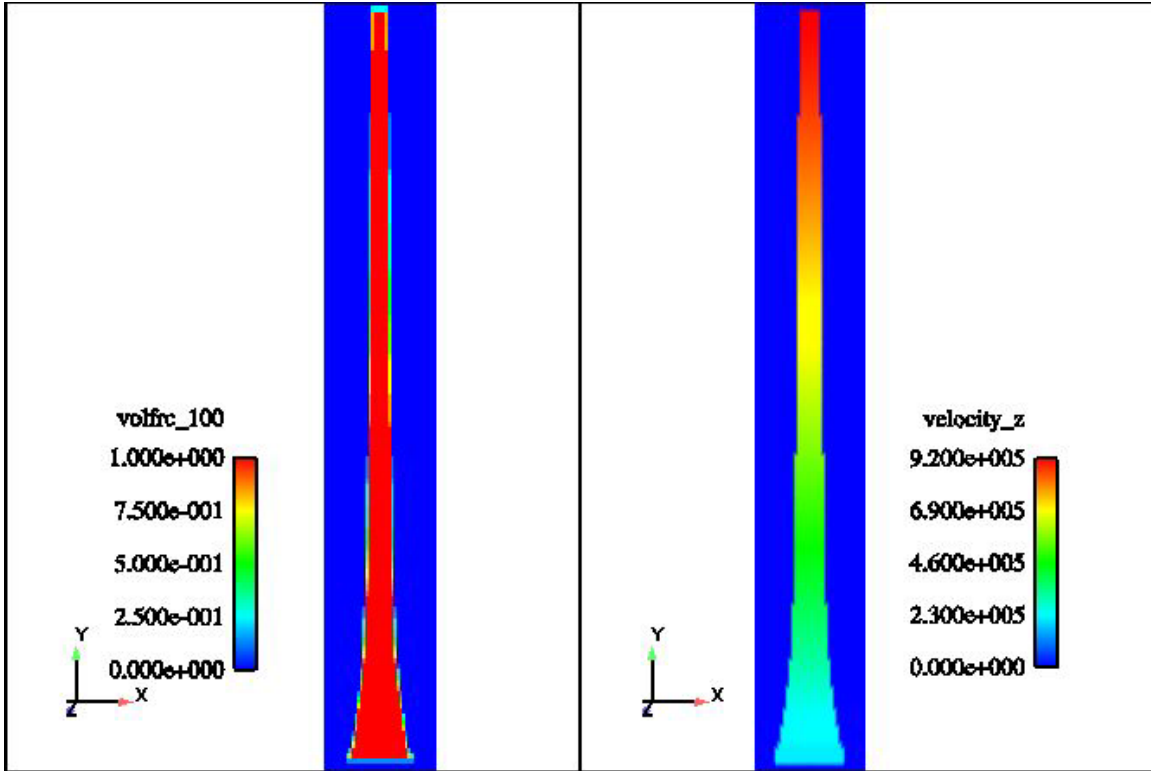


Figure 8. Stretching jet model initial configuration, representing Viper SCJ description at 35 μ s.

Once the baseline model was run, various meshes of different aspect ratio and refinement were studied, to determine their impact on jet tip velocity and particulation characteristics. The particulation of SCJs is discussed in detail in Walters and Zukas (1989) by stating the contributions of many authors toward developing a better understanding of the phenomenon. The length of the stretching jet directly influences the penetration depth achieved once it hits a target; however, penetration starts to decrease significantly when the jet starts to particulate. Hence, it is important for a computational model to represent jet particulation characteristics. Currently, computational jet particulation is largely, if not completely, due to numerical error propagation. Whether the analyst intends to study a problem involving a particulating jet or not, breakup may be observed, depending on the mesh selected. Since the real jet eventually particulates, and since the physics in currently available codes does not enable the prediction of jet particulation, the computational analyst is faced with a major obstacle, especially if having a particulated jet is an important aspect of the problem being studied. One approach is to achieve particulation using numerical effects by carefully designing the mesh. The sensitivity study conducted during this study, and summarized in this section aims at developing a better understanding of mesh effects on this numerically observed phenomenon, so that analysts can pick the properties of their mesh based on the desired accuracy of various jet characteristics in the end.

Table 2 provides a detailed summary of the meshes studied, along with a schematic representation of the cell geometries and the jet characteristics computed at 85 and 120 μs . The mesh input listed in appendix C-2, using parameters listed in appendix C-3, corresponds to Mesh 1 in table 2. Note that the tip velocity was not preserved in any of the cases. Mesh 3 provided the best preservation of tip speed; however, it produced the worst result for jet breakup time. The best estimate for jet breakup time was achieved using Mesh 1. All the meshes, except for Meshes 6 and 7, resulted in jet particulation.

Table 2. Summary of mesh sensitivity investigations using the stretching jet model in ALEGRA.

Mesh	Δy (cm)	Δx (cm)	Aspect Ratio $\Delta y/\Delta x$	Cell Geometry	Min # of Cells per Radius (at the tip)	Max # of Cells per Radius (at the tail)	Jet Breakup Time (μs)	Results at 85 μs			Results at 120 μs		
								Tip Velocity (km/s)	Jet Length (cm)	# of Particles	Tip Velocity (km/s)	Jet Length (cm)	# of Particles
1	0.10	0.05	2.00		3	11	85	8.93	47.8	2	8.92	71.2	18
2	0.05	0.05	1.00		3	11	70	8.98	47.7	20	8.98	71.4	26
3	0.02	0.03	0.50		4	18	65	9.04	47.9	25	9.04	71.8	41
4	0.02	0.02	1.00		7	29	84	8.99	47.9	4	8.98	71.5	33
5	0.01	0.03	0.44		5	23	50	8.99	47.8	21	n/a	n/a	n/a
6	0.10	0.03	4.00		5	22	No particulation up to 150 μs	8.96	47.9	0	8.89	71.2	0
7	0.10	0.01	8.00		10	45	No particulation up to 150 μs	8.97	47.9	0	8.92	71.4	0

Considering the meshes that produced jet particulation, the number of particles numerically formed was less than the experimentally observed number of particles. According to the ARL experimental results shown in figure 1, first particulation was observed at approximately 90 μs . Hence, the number of particles at 85 μs should be 0. At 120 μs , however, there should be 55 particles. Mesh 3 came closest to matching this number, with 41 particles; whereas, Mesh 2 produced only 18 particles.

The mesh sensitivity study summarized in table 2 can be used to form some trends and develop guidelines for selecting cell size and aspect ratio in future studies. However, these trends should not be regarded as conclusive, but only as indicative, since the number of meshes studied was limited. The validity of these trends should be further investigated through additional numerical tests.

Note that there are two square meshes considered. The coarser mesh was 0.05 by 0.05 cm and the refined mesh was 0.02 by 0.02 cm. Based on these two results alone, the jet particulation seemed to be delayed when using refined square mesh, as indicated in figure 9(a). Once the jet started to particulate, the error in the number of particles, calculated at both 85 and 120 μs , was smaller for the refined square mesh, as shown in figure 9(b). Considering the jet breakup times for each mesh, 33 particles at the end of a duration of 36 μs were obtained for the fine mesh; whereas, 26 particles at the end of a duration of 50 μs were obtained for the coarser mesh. In other words, after a late start, more particles were obtained in a shorter amount of time using a finer square mesh; similar to what is observed experimentally. There is no significant difference in the loss in jet tip velocity between the two meshes. Hence, not surprisingly, the more refined square mesh produced better results overall.

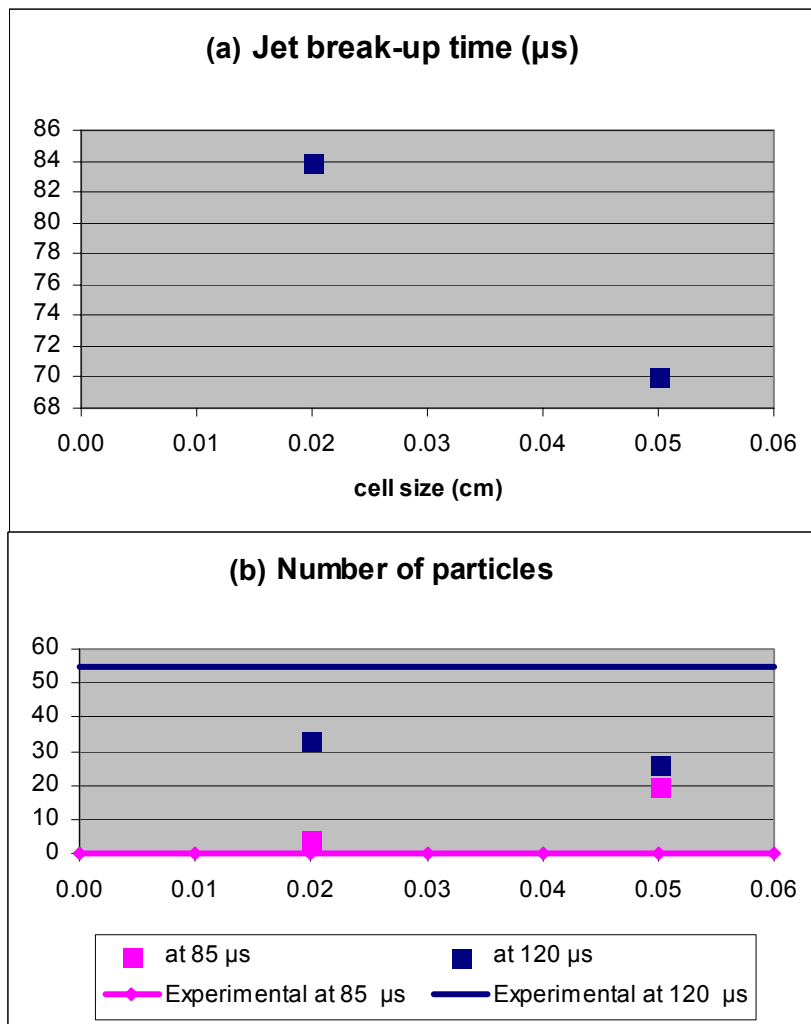


Figure 9. Effect of refinement of a square mesh on (a) jet break-up time and (b) number of particles.

The results summarized in table 2 indicate that as the cell aspect ratio was increased, the jet breakup time also increased, as shown in figure 10. Particulation never occurred for the two highest aspect ratios investigated, i.e. for aspect ratio = 4 and aspect ratio = 8. The earliest jet breakup time occurred for the lowest aspect ratio investigated, 0.44. Note that the cell size was the same in radial direction for the mesh that produced the earliest jet breakup time, and for Mesh 6, with aspect ratio 4 that produced no particulations at all. Approximately the same breakup time was obtained by Meshes 1 and 4. Although Mesh 4 was more refined than Mesh 1, Mesh 1 had twice the aspect ratio of Mesh 4. As the aspect ratio increased, the number of particles obtained decreased, as shown in figure 11. Despite the various different cell sizes, the results were consistent.

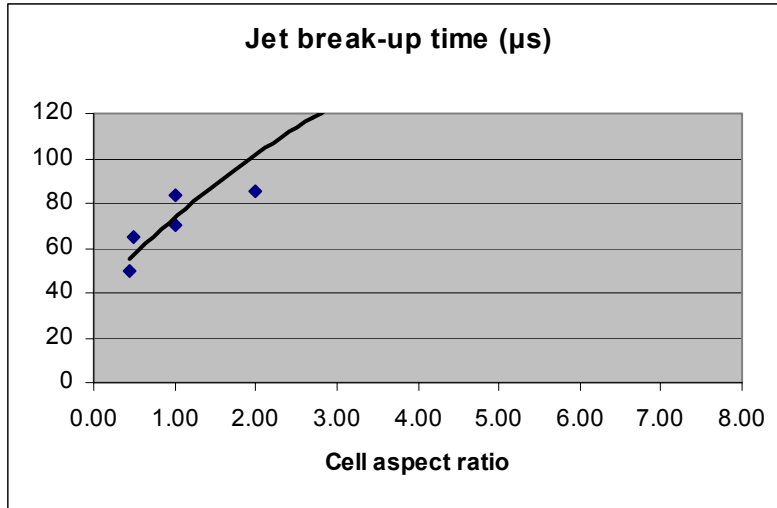


Figure 10. Effect of cell aspect ratio ($\Delta y/\Delta x$) on jet break-up time.

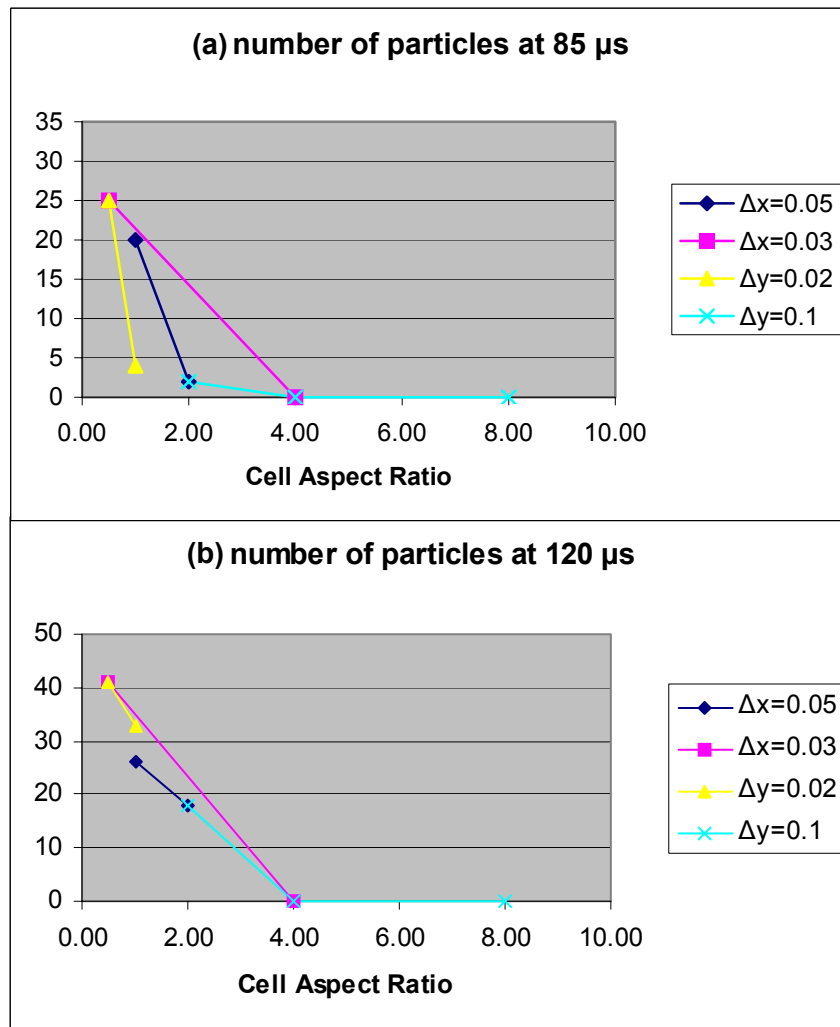


Figure 11. Effect of cell aspect ratio ($\Delta y/\Delta x$) on number of particles formed (a) at 85 μs and (b) at 120 μs .

The difference between the jet tip speeds at 120 μs , obtained using various computational grids, was insignificant; however, the jet tip speed was reduced for all the meshes considered. The worst result, in terms of maintaining the initially specified jet tip speed, was obtained for aspect ratio = 2 and the best result obtained was for aspect ratio = 0.5, as shown in figure 12. However, the best result corresponded to a 1.7% drop in tip speed, whereas the worst result corresponded to a 2.9% drop in tip speed. Therefore, the comparative trends cannot be considered reliable.

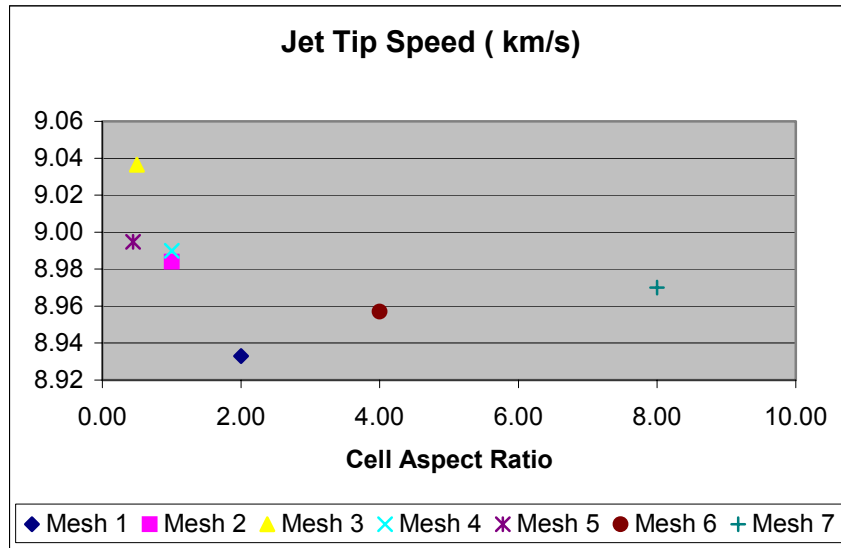


Figure 12. Effect of cell aspect ratio ($\Delta y/\Delta x$) on preserving the jet tip speed.

In terms of matching the experimentally observed jet characteristics, the square mesh labeled Mesh 4 (0.02 by 0.02 cm cells) in table 2 produced the best results. Initially, there were a minimum of 7 cells across the radius at the tip, and 29 cells across the radius at the tail. For this mesh, the error in jet tip speed was 2%, the error in jet breakup time was approximately 7%, the error in jet length at 85 μs was 11%, and the error in number of particles at 120 μs was 40%. The results at 120 μs using this mesh are shown in figure 13. If matching a specific jet characteristic is more important than achieving the overall best response, then changing the cell geometry may reduce the error for one characteristic, while possibly increasing it for another. Note that, the results reported herein are based on ALEGRA version 4.2.

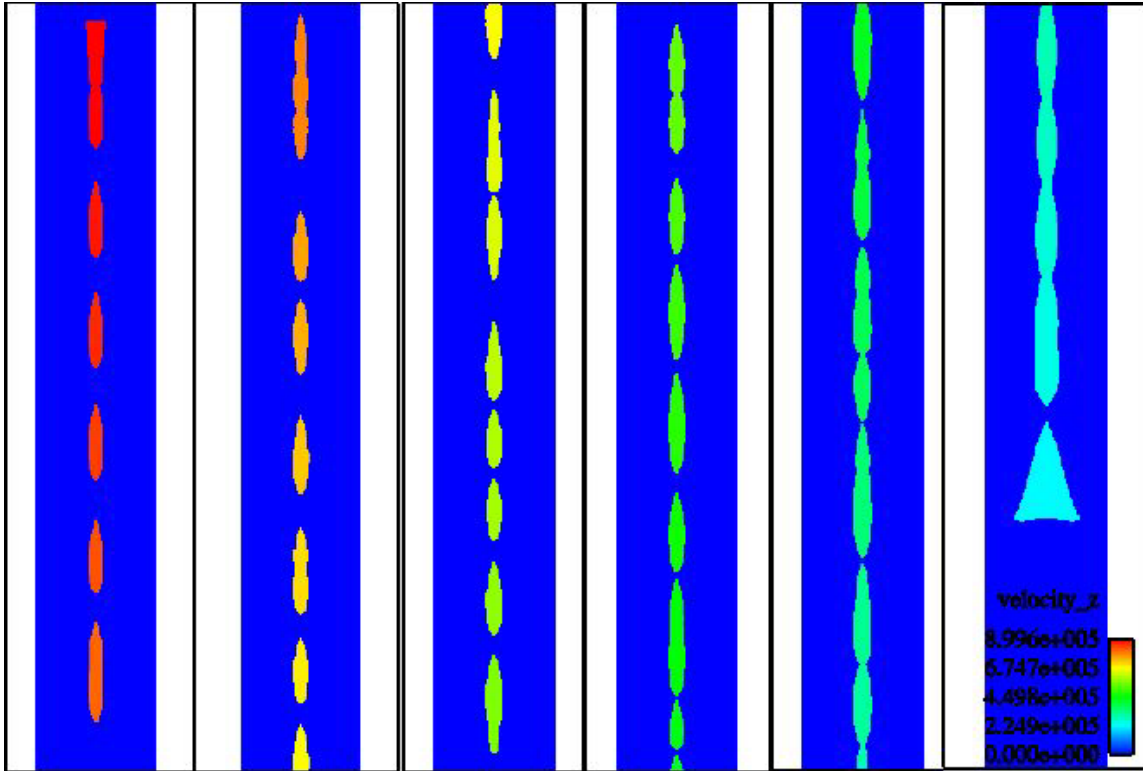


Figure 13. Axial velocity distribution for the particulated jet at 120 μ s.

5. Conclusions

An analytical representation of the geometric shape and axial velocity distribution of a fully formed, stretching Viper SCJ was presented. Computational results were obtained using ALEGRA and were compared to experimental results. The mesh dependency of the jet tip velocity, jet length, breakup time, and the number of particles formed were investigated.

Among various jet characteristics, the jet tip speed and length were found to be the least mesh dependent; whereas, breakup time and number of particles were found to be highly mesh sensitive. The error in jet tip speed was corrected at 35 μ s, which helped reduce the error at 85 μ s from 7% to 2%. Depending on cell geometry, the difference between the experimentally observed and computationally obtained breakup times varied between 6% and 44%. For cells of a higher aspect ratio in the axial direction, the breakup time was delayed and the difference was reduced. However, the number of particles at later times was also reduced, resulting in a greater difference between the experimental data and computational results. For cells with an aspect ratio of 5 and higher, jet particulation did not occur for the duration of computations. The largest error observed for all meshes studied was in estimating the number of particles at 120 μ s; this

value varied between 25% and 67%. Nevertheless, the large errors associated with jet particulation was not a surprising conclusion, since the particulation is due to numerical effects rather than to the physics implemented in the code, as discussed within this report. The results of the mesh sensitivity studies are applicable to SCJ simulations using ALEGRA, and are not confined to the stretching jet model presented in this report.

References

- Blacker, T. D. *FASTQ Users Manual Version 1.2*; SAND88-1326; Sandia National Laboratories: Albuquerque, NM, 1988.
- Boucheron, E. A.; Brown, K. H.; Budge, K. G.; Burns, S. P.; Carroll, D. E.; Carroll, S. K.; Christon, M. A.; Drake, R. R.; Garasi, C. G.; Hail, T. A.; Peery, J. S.; Petney, S. V.; Robbins, J.; Robinson, A. C.; Summers, R. M.; Voth, T. E.; Wong, M. K. *ALEGRA: User Input and Physics Descriptions Version 4.2*; SAND2002-2775; Sandia National Laboratories: Albuquerque, NM, October 2002.
- EnSight User Manual for Version 7.6*. Computational Engineering International, Inc.: 2166 N. Salem St., Suite 101, Apex, NC, 27523, May 2003.
- Johnson, G. R.; Cook, W. H. A Constitutive Model and Data Subjected to Large Strains, High Strain Rates and High Temperatures. *Proceedings of the 7th International Symposium on Ballistics*, The Hague, The Netherlands, 1983.
- G. I. Kerley, G. I. *CTH Reference Manual: The Equation of State Package*; SAND98-0947; Sandia National Laboratories: Albuquerque, NM, 1998.
- Kmetyk, L.N.; Yarrington, P.; Vigil, M.G. *CTH Analyses of Viper Conical Shaped Charges with Comparisons to Experimental Data*; SAND90-2604, Sandia National Laboratories: Albuquerque, NM, January, 1991.
- Lee, E. L.; Hornig, H. C.; Kury, J. W. *Adiabatic Expansion of High Explosive Detonation Products*; UCRL-50422, Lawrence Livermore National Laboratory: Livermore, CA, 1968.
- MATLAB: The Language of Technical Computing, Version 5, The Mathworks Inc., June 1997.
- McGlaun, J. M.; Thompson, S. L.; Elrick, M. G. CTH: A Three-Dimensional Shock Wave Physics Code. *I. J. of Impact Engineering* **1990**, *10*, 351–360.
- Sjaardema, G. D. *GJOIN: A Program for Merging Two or More GENESIS Databases*; SAND92-2290; Sandia National Laboratories: Albuquerque, NM, December, 1992a.
- Sjaardema, G. D. *APREPRO: An Algebraic Preprocessor for Parameterizing Finite Element Analyses*; SAND92-2291, Sandia National Laboratories: Albuquerque, NM, 1992b.
- Thompson, S. L. *Improvements in the CHARTD Radiation-Hydrodynamics Code III: Revised Analytic Equation of State*; SC-RR-710714; Sandia National Laboratories: Albuquerque, New Mexico, March 1972 (ANEOS models).

Thompson, S. L. *Improvements in the CHARTD Energy Flow–Hydrodynamics Code V: 1972/1973 Modifications*; SLA-73-0477; Sandia National Laboratories: Albuquerque, New Mexico, October 1973 (ANEOS extensions).

Walters, W. P.; Zukas, J. A. *Fundamentals of Shaped Charges*, soft cover ed.; CMC Press: Baltimore, MD, 1998.

Acronyms

2-D	two-dimensional
ALE	Arbitrary Lagrangian Eulerian
ALEGRA	Arbitrary Lagrangian Eulerian General Research Application
ANEOS	Analytic Equation of State package
ARL	U.S. Army Research Laboratory
EOS	equation of state
HRIT	High-Resolution Interface Tracker
JWL	Jones-Wilkins-Lee
KEOS	Kerley Equation of State
LANL	Los Alamos National Laboratory
MHD	Magneto-Hydrodynamics
MMALE	Multi-Material Arbitrary Lagrangian Eulerian
SCJ	shaped charge jet
SEACAS	Sandia National Laboratories Engineering Analysis Code Access System

INTENTIONALLY LEFT BLANK.

Appendix A-1. ALEGRA (Version 4.2) Input File Used for Viper SCJ Formation

```
$
$ Title:      2D axisymmetric VIPER shaped charge simulation
$
title
  viper 2d

exodus version two

$

termination time 90.0e-6

emit output: time      = 1.0E-6, from 0.0 to 1.0E-6
emit output: time      = 1.0E-5, from 10.0E-6 to 100.0E-6
emit output: time      = 2.5E-5, from 100.0E-6 to 250.0E-6

emit plot: time        = 1.0E-6, from 0.0 to 20.0E-6
emit plot: time        = 2.5E-6, from 20.0E-6 to 100.0E-6
emit plot: time        = 2.5E-5, from 100.0E-6 to 250.0E-6

emit hisplt: time = 1.0e-6, from 0.0 to 9.0e-5
emit restart: time = 1.0e-6, from 2.0e-5 to 2.3e-5

$ PHYSICS OPTIONS

solid dynamics

cylindrical

$

  programmed burn
    material 2
    detonation point
    x=0.0, y=0.01 at time 0.0
    burn radius 20.0
  end

$

  domain
    smyra interface tracker
    voided sideset 2
    remesh iterations 10
  end

$

  block 1
    add diatom input
```

```

    eulerian mesh
    remesh frequency 1
end

$ BOUNDARY CONDITIONS

no displacement: nodeset 1 x

$ MATERIAL INSERTION

diatoms

package 'CU LINER - 2'
material 1
numsub 50
insert circle
    center 0.0 5.77550
    radius 0.64516
endinsert
delete circle
    center 0.0 5.77550
    radius 0.52578
enddelete
delete box
    p1 0.0 5.588
    p2 0.59817 9.0
enddelete
endpackage

$
package 'CU LINER - 1'
material 1
numsub 50
insert uds
    p1 0.0 12.31392
    p2 0.0 5.58800
    p3 0.59817 5.58800
    p4 3.26009 12.11580
    p5 3.26009 12.31392
endinsert
delete uds
    p1 0.0 12.21486
    p2 0.0 5.58800
    p3 0.483607 5.58800
    p4 3.16103 12.21486
enddelete
delete box
    p1 0.0 12.21486
    p2 3.16103 12.50000
enddelete
endpackage

$
package 'EXPLOSIVE'
material 2
numsub 50
insert uds
    p1 0.0 0.0
    p2 1.59385 0.0

```

```

    p3  3.22834  5.40233
    p4  3.26009 12.11580
    p5  0.0      12.11580
endinsert
delete uds
    p1  0.0      5.588
    p2  0.55880  5.5880
    p3  3.26009 12.11580
    p4  0.0      12.11580
enddelete
delete circle
    center  0.0  5.77550
    radius  0.64516
enddelete
endpackage
enddiatoms

end

$ EXECUTION CONTROL

plot variable
artificial viscosity
pressure
stress
strain
velocity
density
temperature
detonation time
eqps
yield stress
end

$ MATERIAL MODELS

$ MATERIAL 1

material 1      "COPPER"
    model = 1  $ copper eos
    model = 2  $ constitutive
    model = 3  $ fracture
    density 8.94 $ g/cm3
    temperature 298.0 $ Kelvin
end

model 1 keos sesame
    neos  3331
    feos  'aneos'
end

model 2 elastic plastic
    youngs modulus  1.2e+12 $ dyne/cm^2
    poissons ratio  0.33
    yield stress    3.5e+9  $ dyne/cm^2
    hardening modulus 0.0
    beta 1.0

```

```
end

model 3 frac presdep
  init frac pres = -15.0e9
end

$ MATERIAL 2

material 2      "LX-14"
  model = 5
  density 1.835  $ g/cm3
  temperature 298.0 $ Kelvin
end

model 5 programmed burn jwl
  rho ref      1.835
  tref         298.0
  a            11.65e12
  b            0.5572e12
  c            0.01844e12
  omega        0.45
  r1           5.40
  r2           2.0
  pcj          0.360e12
  dcj          0.88e6
  tcj          3970.0
end

$

exit
```

Appendix A-2. Part 1 of Mesh Used to Simulate Shaped Charge Detonation, Liner Collapse, and Jet Formation

```
$ APREPRO ($Revision: 1.69 $)

$
$ Part 1 of mesh for
$ shaped charge detonation jet formation
$
title
meshpart1forshapchardetandjetformtn
$
$ point definitions
$
$
point 1 0 -10
point 2 1 -10
point 3 10 -10
point 4 10 20
point 5 1 20
point 6 0 20
$
$ line definitions
$
line 1 str 1 2 0 25 1.0
line 2 str 2 3 0 180 1.0019
line 3 str 3 4 0 750 1.0
line 4 str 5 4 0 180 1.0019
line 5 str 6 5 0 25 1.0
line 6 str 1 6 0 750 1.0
$
$ region definitions
$
$region 1 1 -1 -2 -3 -4 -5 -6
$region 2 1 -5 -7 -8 -9
$
region 1 1 -1 -2 -3 -4 -5 -6
$
$ boundary conditions
$
nodebc 1 6
elembc 2 1 2 3 4
$
exit
```

INTENTIONALLY LEFT BLANK.

Appendix A-3. Part 2 of Mesh Used to Simulate Shaped Charge Detonation, Liner Collapse, and Jet Formation

```
$ APREPRO ($Revision: 1.69 $)

$
$ Part 2 of mesh for
$ shaped charge detonation jet formation
$
title
meshpart2forshapchardetandjetformtn
$
$ point definitions
$
$
$point 1 0 -10
$point 2 2 -10
$point 3 10 -10
$point 4 10 20
point 5 1 20
point 6 0 20
point 7 1 120
point 8 0 120
$
$ line definitions
$
line 5 str 6 5 0 25 1.0
line 7 str 5 7 0 3000 1.0
line 8 str 8 7 0 25 1.0
line 9 str 6 8 0 3000 1.0
$
$ region definitions
$
$region 1 1 -1 -2 -3 -4 -5 -6
region 2 1 -5 -7 -8 -9
$
$
$ boundary conditions
$
nodebc 1 9
elembc 2 7 8
$
exit
```

INTENTIONALLY LEFT BLANK.

Appendix B-1. MATLAB Program to Determine the Jet Shape at 35 μ s, Using Extracted Data from ALEGRA Calculations

```
% MATLAB
%
% Program to extract material boundary
% Example : boundary of a shaped charge jet
% To use this program, following is needed:
% Series of numbered files (Ex: velgeo1, velgeo2, ...,velgeo25)
% that contain 5 columns of data, preceded by 5 comment lines to be skipped
% based on an output from ensight7.
%
% 5 columns of data are:  volumefraction of copper, velocity_z, x, y, z
% where x is constant in each file, since the files are generated
% using a line tool along the y axis at constant x.  z is always zero.
%
% Input filename without the number as a string
filenamebase=input('What is the filename (without the number) ? ','s');
%
% Input number of files
n=input('How many files ? ');
%
k=0;
bk=0;
%
for i=1:n
    istr=num2str(i);
    filename=strcat(filenamebase,istr);
    f1=fopen(filename);
%
    for j=1:6
        fgets(f1);
    end
%
    arrayname=strcat('a',istr)
    a=fscanf(f1,'%e %e %e %e %e',[5 inf]);
    a='a';
    size_a=size(a);
    size_a=size_a(1,1);
%
    for j=1:size_a
        if a(j,1) >= 0.5
            k=k+1;
            c(k,1)=a(j,3);
            c(k,2)=a(j,4);
            c(k,3)=a(j,2);
            if j > 1  j < size_a
                if (a(j-1,1) < 0.5  a(j+1,1) >= 0.5) | (a(j-1,1) >= 0.5
a(j+1,1) < 0.5)
                    bk=bk+1;
                    B(bk,1)=a(j,3);
                    B(bk,2)=a(j,4);
            end
        end
    end
end
```

Appendix B-2. The Viper Jet Boundary at 35 μ s

Radial Coordinate x (cm)	Axial Coordinate y (cm)
0	13.28
0	27.8636
0.04	13.28
0.04	27.8631
0.08	13.28
0.08	27.8925
0.12	13.28
0.12	23.497
0.12	26.4077
0.12	27.8925
0.16	13.28
0.16	23.497
0.16	26.4077
0.16	27.8925
0.2	13.28
0.2	17.0728
0.2	27.7014
0.2	27.8631
0.24	13.28
0.24	17.0728
0.24	27.7014
0.24	27.8631
0.28	13.28
0.28	15.2793
0.28	27.7014
0.28	27.7308
0.32	13.28
0.32	14.6766
0.32	27.7014
0.32	27.7602
0.36	13.28
0.36	14.6766
0.36	27.7014
0.36	27.7602
0.4	13.28
0.4	13.8386
0.44	13.28
0.44	13.8386
0.48	13.28
0.48	13.5593
0.52	13.28
0.52	13.427
0.56	13.28
0.56	13.3094
0.6	13.28

INTENTIONALLY LEFT BLANK.

Appendix C-1. ALEGRA Problem Specification Deck for the Stretching Jet Model

```
{include(parameters)}
$
$ -----
$ begin execution control section of input
$ -----
$
$
title
2D axisymm viper shaped charge jet representation at 35  $\mu$ s
with an axial velocity function defined along its length
$
$ define stop time/cycle
$
$termination cycle = 1
termination time = 85.0e-06
$
$ output control
$
emit output:      time = 1.0e-06, from 0.0 to 1.0
emit plot:  time = 1.0e-06, from 0.0 to 1.0
emit restart:    time = 10.0e-06, from 0.0 to 1.0
emit hisplt:     time = 1.0e-06, from 0.0 to 1.0
$
$ define variables written to exodus file(s)
$
plot variable
  pressure: avg
  density:  avg
  temperature:  avg
  velocity
  stress
  strain
  yield stress
  eqps
  stretch
  sound speed
  mass
  el mass
end
$
$ -----
$ begin physics section of input
$ -----
$
$
solid dynamics
  $
  $ define the geometry
  $
  cylindrical
  $
  $ controls applied to the entire computational domain
```

```

$
domain
  smyra interface tracker
  voided sideset {bc_exterior}
end
$
$ boundary conditions
$
no displacement: nodeset {bc_symmetry} x
$
$ tracers
$
tracer points
  eulerian tracer 1 x=0.0 y={jet_tail_coordinate}.
  eulerian tracer 2 x=0.0 y={jet_tail_coordinate+0.25*jet_length}
  eulerian tracer 3 x=0.0 y={jet_tail_coordinate+0.50*jet_length}
  eulerian tracer 4 x=0.0 y={jet_tail_coordinate+0.75*jet_length}
  eulerian tracer 5 x=0.0 y={jet_tip_coordinate}
end
$
$ controls for the mesh blocks
$
block 1
  eulerian mesh
  add diatom input
end
$
$ material insertion (diatom) inputs
$
diatoms
  package 'copper_jet'
  material={copper*100}
  agraded p1=0.0 {jet_tail_coordinate}. p2=0.0 {jet_tip_coordinate}
  mvelocity=0.0 T1
  iteration=3
  insert uds
p{i}= 0.0 {jet_tail_coordinate}
p{i+=1}= {jet_radius} {jet_tail_coordinate}
{Loop(no_of_segments)}
  p{i+=1}= {jet_radius-=delta_radius} {-4644.2*(jet_radius**5) +
10582.*(jet_radius**4) - 9473.5*(jet_radius**3) + 4176.8*(jet_radius**2) -
915.87*(jet_radius) + 81.852}
{EndLoop}
p{i+=1}= 0.0 {jet_tip_coordinate}
  endi
  endp
enddiatom
$
$ function 1: axial velocity along length of jet
$
function 1
{Loop(no_of_segments)}
{dist_fr_tail+=delta_length} {0.6261*(dist_fr_tail**5) -
42.871*(dist_fr_tail**4) + 838.*(dist_fr_tail**3) - 7904.5*(dist_fr_tail**2)
+ 93790.*(dist_fr_tail) + 182688. }
{EndLoop}
end

```

```

$
$ this end completes the physics section of the input
$
end
$
$ -----
$ begin material modeling section of input
$ -----
$
$ material definition for copper jet
$
material {copper*100} "COPPER in EOS_data file"
      model {copper*100}
end
$
model {copper*100} cth elastic plastic
  eos model      = {copper*100+1}
  yield model    = {copper*100+2}
  poissons ratio = 0.3
end
$
model {copper*100+1} keos sesame
  datafile = 'EOS_data'
  matlabel = 'COPPER'
end
$
model {copper*100+2} johnson cook ep
  ajo = 8.970000E+08
  bjo = 2.918700E+09
  cjo = 2.500000E-02
  mjo = 1.090000E+00
  njo = 3.100000E-01
  tjo = 1380.718   $1.189813E-01 ev
end
$
$ constitutive model
$ elastic plastic (Copper)
$model,{copper*100},elastic plastic
$youngs modulus = 1.076e+12
$poissons ratio = 0.355
$yield stress = 6.0e+09
$hardening modulus = 2.0e+09
$beta=0.5
$end
$
$ EOS Mie-Gruneisen
$model      {copper*100+1} keos miegruneisen
$      matlabel = 'COPPER'
$end
$
$ pressure dependent fracture
$ model {copper*100+2} frac presdep
$ init frac pres = -5.e10
$ density tolerance = 1.e-6
$ pressure tolerance = 1.e+2
$ end
$

```

```
$  
exit
```

Appendix C-2. APREPRO File to Create a Mesh with the FASTQ Tool

```
{include(parameters)}
$
$ simulation of a copper jet with an initial velocity gradient imposed
$ along its length
$
title
copper jet with velocity gradient along its length
$
$ point definitions
$
point 1 {domain_xmin} {domain_ymin}
point 2 {domain_xmax} {domain_ymin}
point 3 {domain_xmax} {domain_ymax}
point 4 {domain_xmin} {domain_ymax}
$
$ line definitions
$
line 1 str 1 2 0 {nx} 1.0
line 2 str 2 3 0 {ny} 1.0
line 3 str 3 4 0 {nx} 1.0
line 4 str 4 1 0 {ny} 1.0
$
$ region definitions
$
region 1 1 -1 -2 -3 -4
$
$ boundary conditions
$
nodebc {bc_symmetry} 4
elembc {bc_exterior} 1 2 3
$
exit
```

INTENTIONALLY LEFT BLANK.

Appendix C-3. Parameters File Used in Conjunction with the Files Listed in Appendices C-1 and C-2

```
{ECHO(OFF)}
Parameters for simulation of stretching jet

{i=1}

Geometry Parameters
-----
{jet_tip_radius=0.14}
{jet_tail_radius=0.6}
{jet_length=-4644.2*(jet_tip_radius**5) + 10582.*(jet_tip_radius**4) -
9473.5*(jet_tip_radius**3) + 4176.8*(jet_tip_radius**2) -
915.87*(jet_tip_radius) + 81.852}

{jet_radius=jet_tail_radius}
{no_of_segments=100}
{delta_radius=(jet_tail_radius-jet_tip_radius)/no_of_segments}

{jet_tip_coordinate=jet_length}
{jet_tail_coordinate=0.0}
{dist_fr_tail=jet_tail_coordinate}
{delta_length=jet_length/no_of_segments}

Initial Conditions
-----
{jet_tip_velocity=0.6261*(jet_length**5) - 42.871*(jet_length**4) +
838.*(jet_length**3) - 7904.5*(jet_length**2) + 93790.*(jet_length) +
182688.}
{jet_tail_velocity=182688.}

Boundary Conditions
-----
{bc=int(0)}
{bc_symmetry=++bc}
{bc_exterior=++bc}

Material Parameters
-----
{material=int(0)}
{copper=++material}

Grid Parameters
-----
{domain_xmin=0.0}
{domain_xmax=1.0}
{domain_ymin=-1.0}
{domain_ymax=100.0}
{deltax=0.05}
{deltay=0.1}
{domain_x_length=domain_xmax-domain_xmin}
{domain_y_length=domain_ymax-domain_ymin}
```

```
{nx=int(domain_x_length/deltax)}  
{ny=int(domain_y_length/deltay)}  
  
{ECHO (ON) }
```

Distribution List

Copies

- 1 (PDF) DEFENSE TECHNICAL
INFORMATION CTR
DTIC OCA
8725 JOHN J KINGMAN RD
STE 0944
FT BELVOIR VA 22060-6218
- 1 COMMANDING GENERAL
US ARMY MATERIEL CMD
AMCRDA TF
5001 EISENHOWER AVE
ALEXANDRIA VA 22333-0001
- 1 INST FOR ADVNCD TCHNLGY
THE UNIV OF TEXAS
AT AUSTIN
3925 W BRAKER LN STE 400
AUSTIN TX 78759-5316
- 1 US MILITARY ACADEMY
MATH SCI CTR EXCELLENCE
MADN MATH
THAYER HALL
WEST POINT NY 10996-1786
- 1 DIRECTOR
US ARMY RESEARCH LAB
IMNE-AD-IM-DR-R
2800 POWDER MILL RD
ADELPHI MD 20783-1197
- 3 DIRECTOR
US ARMY RESEARCH LAB
AMSRD ARL CI OK TL
2800 POWDER MILL RD
ADELPHI MD 20783-1197

Copies

3 DIRECTOR
US ARMY RESEARCH LAB
IMNE-AD-IM-DR T
2800 POWDER MILL RD
ADELPHI MD 20783-1197

ABERDEEN PROVING GROUND

1 DIR USA AMSAA
T THOMPSON

22 DIR USARL
AMSRD WM
T ROSENBERGER
J SMITH
AMSRD WM T
B BURNS
MSRD WM TA
R DONEY
D KLEPONIS
M NORMANDIA
J RUNYEON
M ZOLTOSKI
AMSRD WM TB
P BAKER
AMSRD WM TC
R ANDERSON
R COATES
M FERMEN-COKER (4 copies)
K KIMSEY
D SCHEFFLER
S SCHRAML
B SORENSEN
R SUMMERS
W WALTERS
AMSRD WM TE
J POWELL

ABERDEEN PROVING GROUND

Copies

- 1 DIR USARL
AMSRD ARL CI OK TP
BLDG 4600

- 4 SANDIA NATIONAL LABORATORIES
DOCUMENT PROCESSING MS-0617
PO BOX 5800
R SUMMERS MS0378
M WONG MS0378
ALBUQUERQUE NM 87185-5800

- 1 COMMANDER
US ARMY ARMOR CENTER
ATZK-MW
FT KNOX KY 40121-5000

- 2 COMMANDER
US ARMY AMCOM
AMSRD AMR
W MCCORKLE
M SCHEXNAYDER
REDSTONE ARSENAL AL 35898-5000

- 2 COMMANDER
US ARMY AMCOM
AMSRD AMR PSWF
G JOHNSON
D KIELSMEIER
REDSTONE ARSENAL AL 35898-5000

- 1 COMMANDER
US ARMY ARDEC
AMSRD AAR TDC
J HEDDERICH
PICATINNY ARSENAL NJ 07806-5000

- 4 COMMANDER
US ARMY ARDEC
AMSRD AAR AEM
S MUSALLI
E LOGSDON
A SEBASTO
M PALATHINGAL
PICATINNY ARSENAL NJ 07806-5000

Copies

3 PROJECT MANAGER
MANEUVER AMMUNITION SYSTEMS
SFAE AMO MAS LC
R DARCY
D GUZIEWICZ
SFAE AMO MAS
W SANVILLE
PICATINNY ARSENAL NJ 07806-5000

1 COMMANDER
US ARMY NGIC
LANG SCC
W GSTATTENBAUER
220 SEVENTH ST NE
CHARLOTTESVILLE VA 22902-5396

2 COMMANDER
US ARMY RESEARCH OFFICE
J BAILEY
S F DAVIS
PO BOX 12211
RESEARCH TRIANGLE PARK NC
27709-2211

7 COMMANDER
NAVAL SURFACE WARFARE CTR
DAHLGREEN DIVISION
H CHEN
D L DICKINSON CODE G24
C R GARRETT CODE G22
W E HOYE G22
T SPIVAK G22
P WALTER
L F WILLIAMS CODE G33
17320 DAHLGREEN RD
DAHLGREEN VA 22448

TOTAL: 62